

Observation of strong red photoluminescence with broadband in indium oxynitride nanoparticles

T. S. Ko, C. P. Chu, H. G. Chen, T. C. Lu, H. C. Kuo, and S. C. Wang

Citation: *Journal of Vacuum Science & Technology A* **24**, 1332 (2006); doi: 10.1116/1.2198863

View online: <http://dx.doi.org/10.1116/1.2198863>

View Table of Contents: <http://scitation.aip.org/content/avs/journal/jvsta/24/4?ver=pdfcov>

Published by the AVS: Science & Technology of Materials, Interfaces, and Processing

Articles you may be interested in

[A comparative study of the sol-gel synthesized nanostructured SnO₂ powders](#)

AIP Conf. Proc. **1536**, 159 (2013); 10.1063/1.4810149

[Synthesis and characterization of sol-gel derived Cr₂O₃ nanoparticles](#)

AIP Conf. Proc. **1447**, 341 (2012); 10.1063/1.4710019

[Sol-gel NiFe₂O₄ nanoparticles: Effect of the silica coating](#)

J. Appl. Phys. **111**, 103911 (2012); 10.1063/1.4720079

[Effect of microstructures on nanocrystallite nucleation and growth in hydrogenated amorphous indium–tin–oxide films](#)

J. Appl. Phys. **93**, 1032 (2003); 10.1063/1.1528298

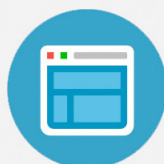
[Ordered indium-oxide nanowire arrays and their photoluminescence properties](#)

Appl. Phys. Lett. **79**, 839 (2001); 10.1063/1.1389071



Re-register for Table of Content Alerts

Create a profile.



Sign up today!



Observation of strong red photoluminescence with broadband in indium oxynitride nanoparticles

T. S. Ko,^{a)} C. P. Chu, H. G. Chen, T. C. Lu, H. C. Kuo, and S. C. Wang

Department of Photonics and Institute of Electro-Optical Engineering, National Chiao Tung University, 1001 Ta Hsueh Road, Hsinchu 30050, Taiwan

(Received 4 May 2005; accepted 27 March 2006; published 22 June 2006)

Indium oxynitride nanoparticles were synthesized on a silicon substrate in nitrogen atmosphere using the method involving thermal evaporation of pure indium in a two-zone reactor. Nanoscale compositional analysis by energy dispersion spectrum showed the existence of indium oxynitride compound. X-ray diffraction analysis further confirmed high crystallization and nitrogen atom existence within the nanoparticles. Scanning electron microscopy investigations showed shape transformation from amorphous sphere to well-shaped octahedron with an average nanoparticle size ranging from 50 nm to 1 μm when the growth temperature of the substrate was increased from 600 to 900 °C. Photoluminescence study was performed on the indium oxynitride nanoparticle samples grown at different temperatures. It was found that with increasing growth temperatures there was not only the formation of high quality indium oxynitride nanoparticles but also an increase in the intensities of emissions. These nanoparticles grown at 900 °C could emit a strong photoluminescence spectrum centered around 700 nm with a broad full width at half maximum of about 250 nm, spanning the whole red segment. © 2006 American Vacuum Society.

[DOI: 10.1116/1.2198863]

I. INTRODUCTION

Transparent conducting oxides are widely used as key components of numerous display and photovoltaic technologies. Many studies of transparent conducting oxides focusing on the synthesis and characterization of structures have experienced a resurgent interest in the past few years. Among these materials, indium oxide, an *n*-type semiconductor with a wide band gap of about 3.6 eV, has been widely employed as microelectronic device material in architectural glasses,¹ solar cells,² sensors,³ and flat-panel displays.⁴ The great possibility in application attracts many researchers to work on this material and some forms of indium oxide, such as films,⁵ powders,⁶ and nanowires,⁷ have been obtained. Recently, Yi *et al.* have grown the polycrystalline $\text{InN}_{1-x}\text{O}_x$ film by the reactive radio frequency magnetron sputtering on Corning 1737 glass substrates.⁸ Contrary to the indium oxide, the syntheses and optical properties of the indium oxynitride have not been studied in detail. In general, ammonia gas was used as the source of nitrides in the chemical vapor deposition (CVD) method. But ammonia and oxygen mixture would cause an explosion at elevated temperature over 700 °C. On the other hand, it is well known that nitrogen with low activity is hard to dissociate by increasing temperature without any assisting method. Therefore, it is difficult to select an appropriate nitrogen atom precursor in preparation of high quality oxynitrides without assisting methods. In this article, we used nitrogen instead of ammonia to synthesize the indium oxynitride nanoparticles on a silicon substrate by using a two-zone CVD technique. Since pyrolysis temperature of nitrogen was greater than 700 °C,⁹ this technique

allowed us to break nitrogen molecules at a high temperature zone (900 °C) and to facilitate the nanoparticle growth in the other downstream zone. In other words, we can adjust the growth temperature to obtain the different dissociation rates of nitrogen in the two-zone CVD reactor. Well-shape octahedron nanoparticles with high crystal quality were observed using this method. In addition, the nanoparticles emitted a broad and strong orange photoluminescence that was different from indium oxide films and powders emitting in blue-green segment. Furthermore, a new red photoluminescence emission band was observed as the growth time was adjusted.

II. EXPERIMENTS

The experimental setup for synthesis of indium oxynitride nanoparticles is depicted schematically in Fig. 1. The starting material, 3 g indium metal, was placed in a quartz boat located inside an 8 cm diameter quartz tube reactor, referred to as zone 1 with the temperature setting as T_1 . *p*-type silicon (100) substrates were placed at the downstream of the tube reactor separated from the starting material by 20 cm, which was referred to as zone 2 with the temperature setting as T_2 . The quartz tube was degassed by a mechanical pump down to 10^{-2} torr and then purged with the nitrogen flow of 150 SCCM (cubic centimeter per minute at STP) as the source of nitrogen atoms. During the growth process, we fixed T_1 to be 900 °C to promote pyrolysis of nitrogen molecules and the indium metal. T_2 in zone 2 was adjusted from 600 to 900 °C. The typical reaction time was about 30 min. The dependence of the reaction time has also been examined and adjusted to 150 min for $T_2=900$ °C. The synthesized nanoparticles on Si substrates were unloaded after the reactor was cooled down. The morphologies and composition of the

^{a)}Electronic mail: tsko.eo93g@nctu.edu.tw

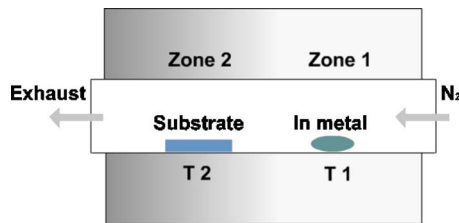


FIG. 1. Schematic diagram of a two-zone CVD system for indium oxynitride nanoparticle growth.

as-grown samples were characterized by field emission scanning electron microscopy (SEM, JEOL 6500F) and energy dispersive x-ray spectrometry (EDS). The structure analysis was also performed by the x-ray diffraction (XRD) measurement with Cu $K\alpha$ radiation. Photoluminescence (PL) spectra were measured at room temperature by means of TRIAX-320 spectrometer using a 25 mW He–Cd laser with the emission wavelength of 325 nm as the excitation source.

III. RESULTS AND DISCUSSION

A typical SEM image of indium oxynitride nanoparticles with well-shape octahedron grown on a Si substrate is shown in Fig. 2(a). This image shows that the dimensions of these

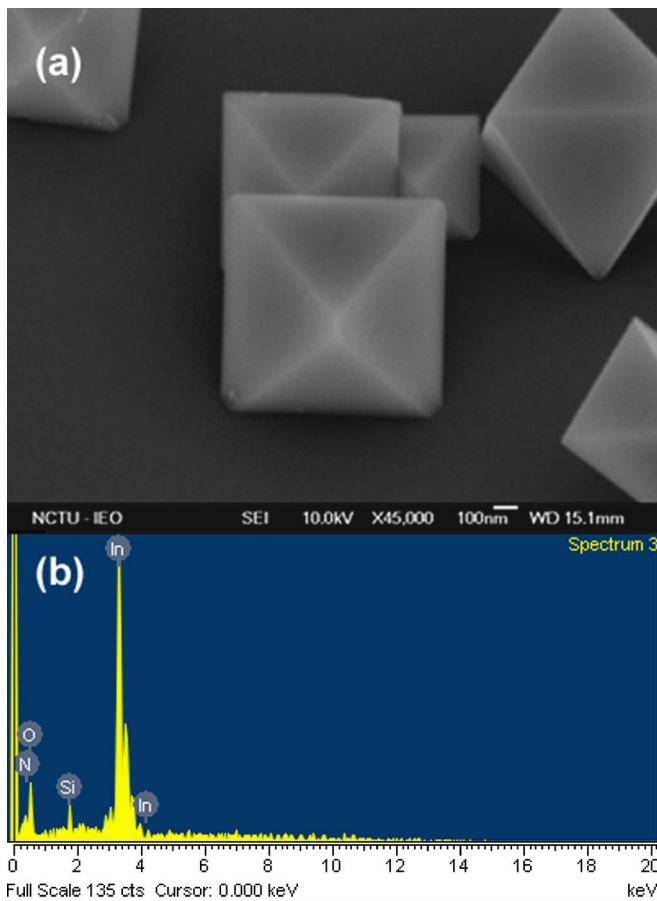


FIG. 2. (a) A typical SEM image of indium oxynitride nanoparticles with well-shape octahedron grown on a Si substrate. (b) EDS results of indium oxynitride nanoparticles.

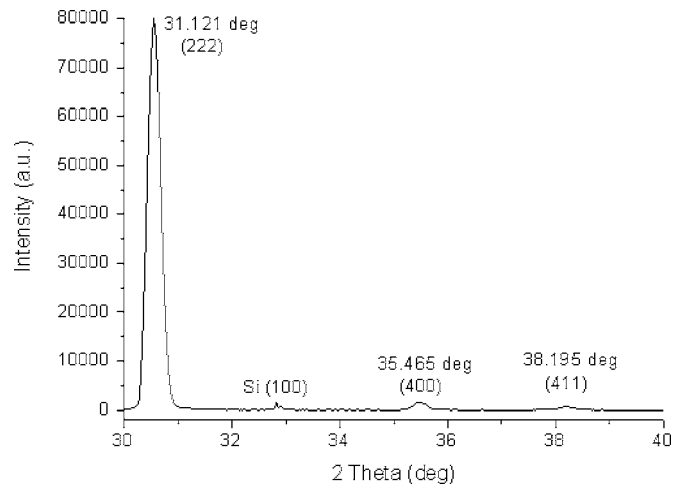


FIG. 3. XRD results of indium oxynitride nanoparticles on Si (100) substrate. The numbers above the peaks correspond to the (hkl) values of the cubic structure.

nanoparticles with well-shaped octahedron range from 500 to 1000 nm, which could relate to the unstable atmosphere and temperature distribution in the reactor. The morphology of nanoparticles is similar to that of the indium oxide nanoparticles reported by Zhang *et al.*¹⁰ As shown in Fig. 2(b), EDS measurement performed on the nanoparticles indicated that the main composition of these nanoparticles was indium. Oxygen and nitrogen could also be identified in the EDS result. However, EDS did not detect nitrogen from the sample grown without placing starting material indium, which indicated that nitrogen atom did not react with Si substrates. Therefore, the formation of indium oxynitride nanoparticles was confirmed by the EDS result.

The typical XRD pattern of the indium oxynitride nanoparticles is shown in Fig. 3. The sharp and symmetric peak at (222) plane implied the crystallization in the indium oxynitride was superior and rather than polycrystalline. All the diffraction peaks could be indexed to a pure cubic phase structure with a lattice constant of $a=0.995$ nm in spite of a little nitrogen incorporation, which was slightly different from the literature value of indium oxide with lattice constant $a=1.011$ nm (JCPDS 71-2195). The (222), (400), and (411) peaks for indium oxide from the standard value (JCPDS 71-2195) are 30.585° , 35.462° , and 37.692° , respectively. Our XRD result showed the (222), (400), and (411) peaks shifted to 31.121° , 35.465° , and 38.195° , which was reasonable when the smaller nitrogen atoms replaced the oxygen atom. Therefore, the lattice constant of indium oxynitride was smaller than the standard value of indium oxide. The XRD results indicated that incorporation of nitrogen was consistent with the EDS analysis. The relatively strong (222) diffraction peak suggested that most crystals were characterized as a (222) plane parallel to the silicon substrate.

In our growth condition, there were a great deal of indium oxynitride octahedral nanoparticles found in the downstream when In chunks were heated at 900°C . The low evaporation pressure of indium even at the high temperature has the ad-

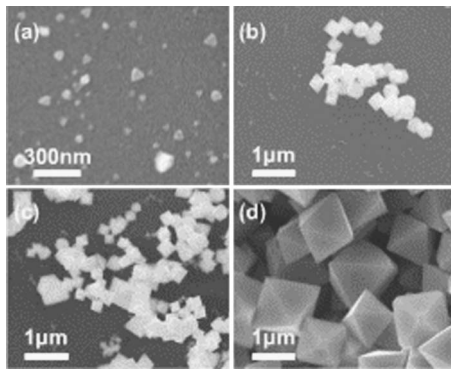


FIG. 4. SEM images of indium oxynitride nanoparticles grown at different temperatures. (a)–(d): 600, 700, 800, and 900 °C.

vantages of one-dimensional nanomaterial growth as reported by Zhang *et al.*¹¹ Since no catalyst on Si substrates was used, we suggested that growth of indium oxynitride octahedrons might be due to the vapor-solid (VS) mechanism. Indium vapor was generated at high temperature and combined with oxygen and nitrogen atoms to form special shaped indium oxynitride and then deposited on the Si substrates at zone 2.

Figures 4(a)–4(d) show the indium oxynitride nanoparticles grown at different temperatures of zone 2 from 600 to 900 °C, respectively. The average size of the nanoparticles gradually increased from 50 nm to 1 μm . The transformation from amorphous to well-shape octahedron with increasing growth temperature can be observed clearly. In addition, the amount of nanoparticles increased and aggregated closer and closer. Two aspects could be considered. First, the indium vapor from zone 1 could gain high thermal energy at 900 °C to bind with oxygen and nitrogen. Then, the formed indium oxynitride deposited on the Si substrates in zone 2. Second, the shape transformation implied that the effect of annealing was notable at the higher growth temperature. In general, crystal structure repair and ion activation often take place during the annealing process. In other words, most defects will be pruned and the quality will be improved after annealing. Therefore, we suggested that the crystal growth and repair occurred at the same time. The photoluminescence spectrum of the indium oxynitride nanoparticles with different growth temperatures was measured at room temperature. Figure 5 shows the strong and broad PL emission spectra from the indium oxynitride nanoparticles with different growth temperatures, which are mainly located in the orange color band with the peak wavelength centered around 610 nm. The emission intensity increased when the samples were grown with increasing temperature, which also suggested that the higher quality indium oxynitride nanoparticles formed at higher temperature.

Moreover, the influence of extending the growth time from 30 to 150 min was investigated when T_1 and T_2 were both at 900 °C. Figure 6 shows the PL spectrum from the indium oxynitride nanoparticles when the growth time was extended to 150 min. A broad PL emission band centered around 700 nm was found with a full width at half maximum

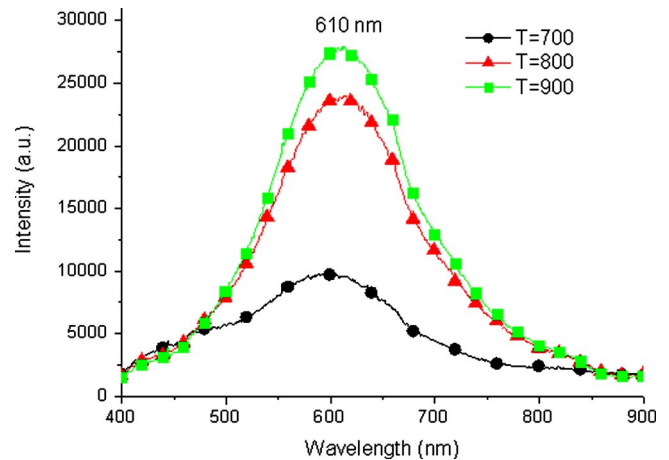


FIG. 5. PL spectra of indium oxynitride nanoparticles grown at different temperatures for 30 min.

(FWHM) of about 250 nm, spanning the whole red segment. The broad FWHM of the PL spectrum could be due to the thermal excitations and the large size distribution of the nanoparticles. Nitrogen flow was found to be very important to grow nanomaterials in this CVD system. Carrier gas frequently affected the morphology and quality of products in similar experiments. However, how the flow affects the morphology in the present work needs further study. In the previous investigations, Zhou *et al.* had reported PL peaks at 480 and 520 nm observed from indium oxide nanoparticles,¹² and Lee *et al.* had reported PL peak at 637 nm observed from indium oxide film.⁵ According to these reports, the emission mechanism was mainly attributed to the effect of the oxygen vacancies. As a result, gradually increasing temperature could make the oxygen vacancies decrease, and decrease the intensity of PL emission. However, the intensity of the PL emission in these indium oxynitride nanoparticles was increased as the growth temperature was increased. Therefore, the emission did not result from the

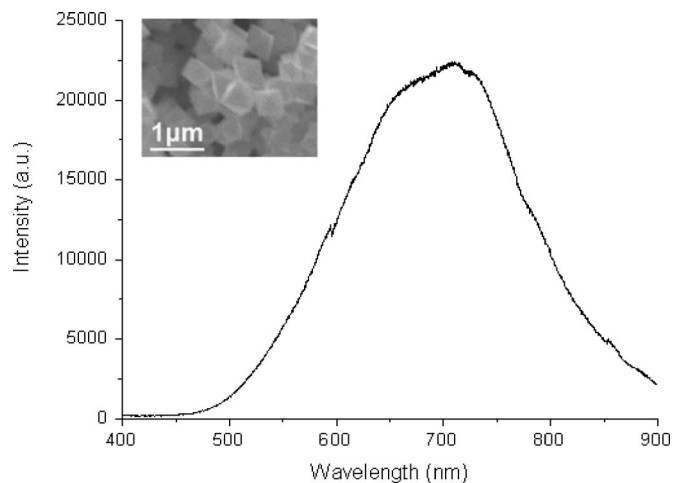


FIG. 6. PL spectrum of indium oxynitride nanoparticles grown at 900 °C for 150 min. The insert SEM image reveals the morphology of the nanoparticles.

radioactive recombination of a photoexcited hole with an electron occupying the oxygen vacancies. The possibility of the observed PL arising from a quantum confinement effect could be also excluded because the exciton Bohr diameter for the indium oxide was estimated to be in the range between 2.6 and 5 nm,¹² which was far smaller than the dimension of these indium oxynitride nanoparticles. To conclude the above contentions, the photon could be emitted by the transition of an excited carrier from the conduction band to the valence band of indium oxynitride nanoparticles along a radiative recombination path. Contrary to the result in Fig. 5, not only the FWHM increased but also the center peak redshifted about 100 nm. The inset figure reveals the SEM image of nanoparticles grown for 150 min. The well-shape octahedron held but the reduced size of nanoparticles to about 300–500 nm could be due to the part dissociation of indium oxynitride causing the slight increase of the N/O ratio of these indium oxynitride nanoparticles when extending the growth time.

IV. CONCLUSION

We have synthesized indium oxynitride nanoparticles by using a thermal evaporation method in a two-zone reactor. EDS and XRD analysis results confirmed the composition and the crystal form of the indium oxynitride compound. SEM investigations showed shape transformation from amorphous sphere to well-shaped octahedron with an average nanoparticle size from 50 nm to 1 μ m when the growth temperature increased from 600 to 900 °C. The room temperature PL spectra of the nanoparticles with different growth temperatures showed light emission in the orange

band, which might be related to the band-to-band transition. The PL spectrum could be further stretched to 700 nm with a broad FWHM of about 250 nm, spanning the whole red segment when the indium oxynitride was grown for extended time. The PL results indicated that indium oxynitride nanoparticles have potentials in developing the red phosphor system for lamp applications.

ACKNOWLEDGEMENTS

The authors would like to thank Dr. J. Shieh of National Nano Device Laboratory for helpful suggestions. The work was supported by the National Science Council of the Republic of China (ROC) in Taiwan under Contract Nos. NSC 93-2120-M-009-006, NSC 93-2752-E-009-008-PAE, and NSC 93-2215-E-009-068.

¹Y. Shigesato, S. Takaki, and T. Haranoh, *J. Appl. Phys.* **71**, 3356 (1992).

²I. Hamberg and C. G. Granqvist, *J. Appl. Phys.* **60**, R123 (1986).

³X. Li, M. W. Wanlass, T. A. Gessert, K. A. Emery, and T. J. Coutts, *Appl. Phys. Lett.* **54**, 2674 (1989).

⁴C. G. Granqvist, *Appl. Phys. A: Solids Surf.* **57**, 19 (1993).

⁵M. S. Lee, W. C. Choi, E. K. Kim, C. K. Kim, and S. K. Min, *Thin Solid Films* **279**, 1 (1996).

⁶S. B. Qadri, H. Kim, H. R. Khan, A. Piquè, J. S. Horwitz, D. Chrisey, and E. F. Skelton, *J. Mater. Res.* **15**, 21 (2000).

⁷C. H. Liang, G. W. Meng, Y. Lei, F. Philipp, and L. D. Zhang, *Adv. Mater. (Weinheim, Ger.)* **13**, 1330 (2001).

⁸Y. Yi, S. Cho, Y. Roh, M. Noh, C. N. Whang, K. Jeong, and H. J. Shin, *Jpn. J. Appl. Phys., Part 1* **44**, 17 (2005).

⁹H. Xiao, *Introduction to Semiconductor Manufacturing Technology* (Prentice-Hall, Upper Saddle River, NJ, 2001), p. 492.

¹⁰Y. Zhang, H. Ago, J. Liu, M. Yumura, K. Uchida, S. Ohshima, S. Iijima, J. Zhu, and X. Zhang, *J. Cryst. Growth* **264**, 363 (2004).

¹¹Y. J. Zhang, N. L. Wang, S. P. Gao, R. R. He, S. Miao, J. Liu, J. Zhu, and X. Zhang, *Chem. Mater.* **14**, 1654 (2002).

¹²H. J. Zhou, W. P. Cai, and L. D. Zhang, *Appl. Phys. Lett.* **75**, 495 (1999).